Computer Aided Geometric Design 34 (2015) 37–49

Contents lists available at ScienceDirect

Computer Aided Geometric Design

www.elsevier.com/locate/cagd

Scattered data interpolation with nonnegative preservation using bivariate splines and its application ☆

Ming-Jun Lai [a,*], Christof Meile [b]

[a] Department of Mathematics, The University of Georgia, Athens, GA 30602, United States of America
[b] Department of Marine Sciences, The University of Georgia, Athens, GA 30602, United States of America

ARTICLE INFO

Article history:
Received 29 April 2014
Received in revised form 16 January 2015
Accepted 20 February 2015
Available online 5 March 2015

Keywords:
Bivariate splines
Scattered data interpolation
Nonnegative preserving

ABSTRACT

We study how to use bivariate splines for scattered data interpolation with nonnegativity preservation of the given data values. That is, we propose a constrained minimal energy method to find a C^1 smooth interpolation of nonnegative data values over scattered locations using bivariate splines. We establish the existence and uniqueness of the minimizer under mild assumptions on the data locations and triangulations. Next we show some approximation properties of the minimizer. We then use the classic projected gradient algorithm to find the minimizer using a simplified nonnegative constraint. Some synthetic as well as a real life example demonstrate the performance, producing nonnegative interpolatory spline surfaces from nonnegative data values. Experimental results also show that the approximation of the nonnegative interpolatory spline surfaces is slightly better than the approximation of the classic minimal energy interpolatory splines.

1. Introduction

Bivariate splines are smooth piecewise polynomial functions over a triangulation $\triangle$ which can be used to find a smooth interpolation to scattered data. Many approximation properties of such interpolatory and fitting splines have been studied (cf. e.g. Lai, 2008). In this paper, we explore how to find an interpolatory spline which preserves its nonnegativity and has some approximation property. Many computer aided design problems require fitting surfaces with nonnegative constraints for visualization of scattered data and/or for surface control. It also emerges in the study of data fitting problems on population or concentration data, as exemplified in the quantification of oxygen anomalies in the deep ocean following the Deepwater Horizon oil spill (see Section 4.2). In general, given a set of data $\{(x_i, y_i, z_i); i = 1, \ldots, N\}$, one wishes to construct a surface S which resembles the given data in the following senses:

1) if the data values z_i are obtained from a smooth function f, i.e. $z_i = f(x_i, y_i)$, then S should be smooth;
2) if the data values are nonnegative, so is S;
3) if the data exhibit a monotone property, then S should have similar monotone property;
4) if data values are from a convex function or the data have a convex property, e.g., the piecewise linear interpolant is convex, then S should also be convex;
5) if the data values vary within a range, then the values of S should be also within the same range;

☆ This paper has been recommended for acceptance by Larry Schumaker.

* Corresponding author.
E-mail address: mjlai@math.uga.edu (M.-J. Lai).

http://dx.doi.org/10.1016/j.cagd.2015.02.004
0167-8396/

6) if the data values are from a smooth function f, then S should approximate f when the number of data locations and values increases.

Note that the requirement 6), i.e. the data fidelity is the most important requirement in the data fitting problem.

As the data values are scattered over a domain of irregular shape, it is convenient to use triangulation based methods for data interpolation. Let $\triangle$ be a triangulation of a domain which contains all data locations $\{(x_i, y_i, z_i); i = 1, \dots, N\}$, for which we can define bivariate splines as follows: For two positive integers $r \geq 1$ and $d > r$,

$$S_d^r(\triangle) := \{s \in C^r(\Omega) : s|_t \in \mathbb{P}_d, \forall t \in \triangle\} \tag{1}$$

is the bivariate spline space of smoothness r and degree d over triangulation $\triangle$, where $\mathbb{P}_d$ is the space of all polynomials of total degree $\leq d$ and $t \in \triangle$ stands for a triangle in $\triangle$. For convenience, let us assume Ω is a closed set. Piecewise bivariate polynomial functions over a triangulation are efficient for computation. It is known that $S_d^r(\triangle)$ can be used to approximate any function in $C^1(\Omega)$ as the size $|\triangle|$ of the triangulation goes to zero, where $|\triangle|$ is the length of the longest edge of $|\triangle|$ (cf. Lai and Schumaker, 2007). Therefore, we adopt these functions to approximate the given nonnegative data values. We refer to Lai and Schumaker (2007) for the theory on bivariate splines and to Awanou et al. (2006) and Lai and Schumaker (2009) for computations with bivariate splines. A classic approach to find the data interpolatory splines is to use the minimal energy method satisfying the data resemblance requirements 1) and 6): That is, one looks for

$$\min_{s \in C^1(\Omega)} \{E(s) : \quad s(x_i, y_i) = z_i, i = 1, \cdots, N\}, \tag{2}$$

where Ω is a closed polygonal domain containing data locations, $C^1(\Omega)$ is the collection of all continuously differentiable functions over Ω, and $E(s)$ is the well-known thin-plate energy functional

$$E(s) = \int_\Omega \left(|D_x^2 s|^2 + 2|D_x D_y s|^2 + |D_y^2 s|^2 \right) dxdy.$$

Here D_x and D_y stand for partial derivatives with respect to x and y. As $C^1(\Omega)$ is an infinitely dimensional space, we use bivariate splines to approximate the minimizer in (2) by considering the following minimization:

$$\min_{s \in S_d^r(\triangle)} \{E(s) : \quad s(x_i, y_i) = z_i, i = 1, \cdots, N\}, \tag{3}$$

where $r \geq 1$ and $\triangle$ is a triangulation of Ω. See Awanou et al. (2006) for numerical solution of (3) and Von Golitschek et al. (2002) for approximation property of the minimizer of (3) which is called minimal energy interpolant. To construct positive preserving interpolatory splines fulfilling data resemblance requirements 1) and 2), Schumaker and Speleers proposed an algorithm to use C^1 quadratic splines based on Powell–Sabin refinement of a triangulation of the given data locations (Schumaker and Speleers, 2010), assuming nonnegative data values and known gradient vectors at all locations. Similarly, they proposed algorithms using the C^1 cubic spline space on the Clough–Tocher refinement of a triangulation of the given data locations with additional gradient values, and showed that their nonnegative spline interpolation can approximate a nonnegative function f when the size of triangulation goes to zero. In addition, Schumaker and Speleers (2010) presented an excellent summary of many local schemes to construct nonnegative preserving interpolatory functions and sufficient conditions of polynomials or rational functions to be nonnegative over a triangle. See Saaban et al. (2011) for the performance of several local schemes for interpolatory surfaces with positive preservation. More recent developments of some rational functions for nonnegative preserving interpolation can be found in Hussain and Hussain (2011) and Sarfraz et al. (2012).

In practice, data locations usually do not cover the entire domain evenly. Although one can add more vertices to have a triangulation with better quasi-uniform property, i.e.

$$\frac{|\triangle|}{\rho_\triangle} \leq \beta < \infty \tag{4}$$

where $\rho_\triangle$ is the smallest of the radii of the inscribed circles of all triangles in $\triangle$. The nonnegative preserving schemes mentioned above would require data values at all vertices. In contrast, here, we study the data fitting problem with the resemblance requirements 1), 2) and 6) by formulating the problem in the following minimization problem:

$$\min_{s \in S_d^r(\triangle)} \{E(s) : \quad s(x_i, y_i) = z_i, i = 1, \cdots, N; s(x, y) \geq 0, \forall (x, y) \in \Omega\}. \tag{5}$$

That is, we use a global minimization approach to choose all the spline coefficients except for those which are at the given data locations based on a triangulation with a reasonable quasi-uniform constant β. Note that β appears in the approximation constant (cf. Lai and Schumaker, 2007). The smaller the β the better for the approximation. Certainly, the approach in (5) is not a brand-new approach. See Willemans and Dierckx (1995), Saaban et al. (2011) and Sarfraz et al. (2012).

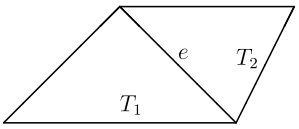

Fig. 1. An interior edge e is active.

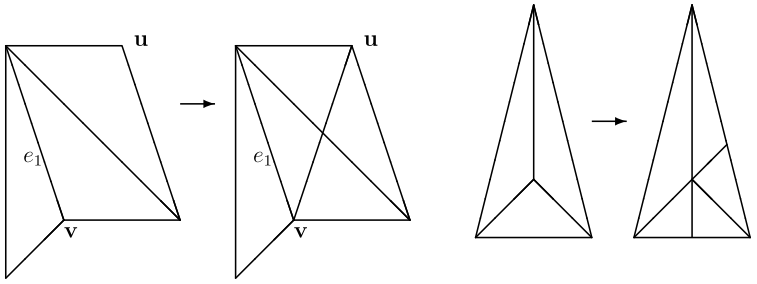

Fig. 2. Conversion of inactive edges e_1 into active edges in two settings.

We shall first show that under some trivial conditions on data locations and a condition on triangulation, the minimization above has a unique solution (see Theorem 2.1 in the next section). We next show that the minimizer $S_z \in S_d^r(\triangle)$ will approximate f if $z_i = f(x_i, y_i)$ for $i = 1, \dots, N$ as $|\triangle|$ goes to zero. Two versions of the approximation property of S_z will be given. One is the convergence under the assumption that f is strictly positive and $|\triangle|$ can be sufficiently small, i.e. we are given a sufficiently amount of data values over locations which are spread out evenly to cover the entire domain. Another version is to show the approximation of S_z for any nonnegative f over any given triangulation. With these preparations, we discuss how to numerically solve this constrained minimization (5). There are many algorithms for constrained minimization problem such as the projected gradient method (cf. Ciarlet, 1989), the Uzawa algorithm (cf. Ciarlet, 1989), the penalty function method and the barrier function method (cf. Nesterov, 2004). In this paper we use the projected gradient algorithm (cf. Ciarlet, 1989). To do so, we use a simplified sufficient condition for the constraint $s(x; y) \geq 0$. Then we establish that our numerical algorithm is convergent (see Theorem 2.5) and apply it to several test cases. Our approach can also be extended to deal with range restricted data interpolation problem. See Example 4.2. In addition, data values often are noisy. Thus, one may also consider penalized least squares data fitting with preservation of nonnegativity, which leads to an unconstrained minimization problem.

2. Main results and proofs

Let us begin with a new concept. We say an interior edge e of triangulation $\triangle$ is *active* if letting $Q_e = T_1 \cup T_2$ be two triangles from $\triangle$ sharing e, the line segment connecting the two tipping vertices of Q_e (two vertices of Q_e which are not in e) intersects e. See Fig. 1 for two triangles T_1, T_2 and e which is an active edge. One can easily change an inactive edge e_1 to an active one by connecting **u** and **v** by a line segment (see Fig. 2, left panel), or introducing new edges (Fig. 2, right panel).

Theorem 2.1. *Assume that the data ($N \geq 3$) are not located on one line. For $r = 1$ and $2 \leq d \leq 4$, we use the Powell–Sabin refinement $\triangle_{PS}$ of $\triangle$ and use $S_d^1(\triangle_{PS})$ for the $S_d^r(\triangle)$ in the minimization (5). For $r = 1$ and $d \geq 5$, we assume that all the interior edges of $\triangle$ are active and we simply use $S_d^1(\triangle)$ for the $S_d^r(\triangle)$ in (5). Then there exists a unique spline $S_z \in S_d^r(\triangle)$ solving the minimization (5).*

Proof. We first show that the feasible set $U = \{s \in S_d^1(\triangle); s(x_i, y_i) = z_i, i = 1, \dots, N; s(x, y) \geq 0\}$ is not empty. For $d = 2$, we can use Algorithm 1 in Schumaker and Speleers (2010) to have a nonnegative spline interpolant S_0. If data values are not given at some vertices of $\triangle$, we simply use any nonnegative values, say 1 for these values. For $d = 3$ and $d = 4$, we know $S_2^1(\triangle_{PS}) \subset S_d^1(\triangle_{PS})$ and hence, U is not an empty set. These show that the feasible set U is nonempty for $2 \leq d \leq 4$ over a Powell–Sabin refinement $\triangle_{PS}$ of a triangulation of the given data locations. For $d \geq 5$, we can construct a nonnegative interpolatory spline $S_f \in S_5^1(\triangle)$ as shown in Fig. 3.

Indeed, one usually uses the Bernstein–Bézier polynomials to express each spline function over the triangulation. That is, in terms of B-coefficients, we can write a spline function $s(x, y)$ as

$$s(x, y) = \sum_{i+j+k=d} c_{ijk}^t B_{ijk}^t(x, y), \text{ if } (x, y) \in t \in \triangle \tag{6}$$

where $\mathbf{c} = (c_{ijk}^t; i + j + k = d; t \in \triangle)$ of size $DT_N \times 1$, and $B_{ijk}^t; i + j + k = d$ are Bernstein–Bézier polynomials of degree d over triangle t (see Chapter 2 in Lai and Schumaker, 2007), $D = (d + 1)(d + 2)/2$ and T_N is the number of total triangles

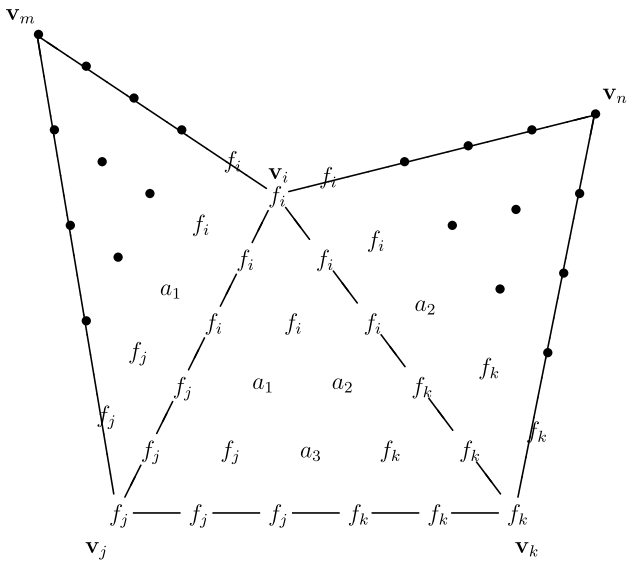

Fig. 3. A construction of nonnegative interpolation.

in $\triangle$. Consider a triangle $T = \langle \mathbf{v}_i, \mathbf{v}_j, \mathbf{v}_k \rangle \in \triangle$. In Fig. 3, we show the B-coefficients of a spline interpolant $S_f \in S_5^1(\triangle)$ over T. First, we immediately see that S_f interpolates f at vertices of $\mathbf{v}_i$, $\mathbf{v}_j$, $\mathbf{v}_k$. It is easy to verify that these coefficients satisfy the C^1 smoothness conditions across edges $[\mathbf{v}_i, \mathbf{v}_j]$ and $[\mathbf{v}_i, \mathbf{v}_k]$. In Fig. 3, the polynomial coefficients c^t_{ijk} are given by $a_1 = \frac{b_1 f_j + b_3 f_i}{1+|b_2|}$, where $\mathbf{v}_m = b_1\mathbf{v}_j + b_2\mathbf{v}_k + b_3\mathbf{v}_i$ with $b_1 + b_2 + b_3 = 1$. Similarly, $a_2 = \frac{c_1 f_i + c_3 f_k}{1+|c_2|}$, where $\mathbf{v}_n = c_1\mathbf{v}_i + c_2\mathbf{v}_j + c_3\mathbf{v}_k$ with $c_1 + c_2 + c_3 = 1$. a_3 is similar to a_1 and a_2 if the edge $\langle \mathbf{v}_j, \mathbf{v}_k \rangle$ is an interior edge. If $\langle \mathbf{v}_j, \mathbf{v}_k \rangle$ is a boundary edge, we let $a_3 = (f_j + f_k)/2$. Since these interior edges $[\mathbf{v}_i, \mathbf{v}_j]$ and $[\mathbf{v}_i, \mathbf{v}_k]$ are active, $b_1 \geq 0$, $b_3 \geq 0$ and $c_1 \geq 0$, $c_3 \geq 0$. Thus all the coefficients over T are nonnegative and hence, S_f on T is a nonnegative polynomial on T. As the spline function S_f is so defined for all triangles in $\triangle$, S_f is a nonnegative interpolant in $S_5^1(\triangle)$. This shows that the feasible set U is nonempty for $d \geq 5$.

Next, we can write $J(\mathbf{c}) := E(s)$ if a spline function s is written in terms of (6). Then it is easy to see $J(\mathbf{c})$ is a continuous function of $\mathbf{c}$. One can show that the boundedness of $\mathbf{c}$ is equivalent to the boundedness of $J(\mathbf{c})$ by using the Markov inequality. $J(\mathbf{c})$ achieves its minimum over the domain of $\mathbf{c}$ such that $J(\mathbf{c}) \leq J(\mathbf{c}_0)$, where $\mathbf{c}_0$ is the coefficient vector of the nonnegative interpolant $S_f \in U$.

Finally we show the minimizer S_z is unique. Otherwise, let us say S_z and S_w are two minimizers. Then $S_\alpha = \alpha S_z + (1-\alpha)S_w$ is also in U for all $\alpha \in (0,1)$ and $E(S_\alpha)$ also achieves the minimum. Then $\frac{\partial d}{d\alpha} E(S_\alpha)|_{\alpha=0_+} = 0$ and $\frac{\partial d}{d\alpha} E(S_\alpha)|_{\alpha=1_-} = 0$ imply

$$\int_\Omega D_x^2 S_w D_x^2 (S_z - S_w) + 2 D_x D_y S_w D_x D_y (S_z - S_w) + D_y^2 S_w D_y^2 (S_z - S_w) = 0$$

and

$$\int_\Omega D_x^2 S_z D_x^2 (S_z - S_w) + 2 D_x D_y S_z D_x D_y (S_z - S_w) + D_y^2 S_z D_y^2 (S_z - S_w) = 0.$$

It follows that $E(S_z - S_w) = 0$. The smoothness condition, i.e. C^1 condition implies that $S_z - S_w$ is a linear polynomial. As the given data set has 3 or more data locations which are not on the same line, the linear polynomial is zero at the data locations and hence, the linear polynomial $S_z - S_w = 0$ or $S_z = S_w$ everywhere on Ω. These complete the proof. □

We next show some approximation properties of S_z. Let $W_\infty^2(\Omega)$ be the space of all twice differentiable functions over Ω with bounded maximum norm of the second order derivatives, that is, $|f|_{2,\infty,\Omega} < \infty$. Next we recall the following approximation property (cf. Lai and Schumaker, 2007).

Theorem 2.2 *(Optimal approximation order). Assume $d \geq 3r + 2$ and let $\triangle$ be a triangulation of Ω. Then there exists a quasi-interpolatory operator $Q(f) \in S_d^r(\triangle)$ mapping $f \in C(\Omega)$ into $S_d^r(\triangle)$ such that $Q(f)$ achieves the optimal approximation order: if $f \in C^{m+1}(\Omega)$,*

$$\|D_1^\alpha D_2^\gamma (Q(f) - f)\|_{C(\Omega)} \leq C|\triangle|^{m+1-\alpha-\gamma} |f|_{m+1,\Omega} \tag{7}$$

for all $\alpha+\gamma \le m+1$ with $0 \le m \le d$, where D_1 and D_2 denote the derivatives with respect to the first and second variables and the constant C depends only on the degree d and the smallest angle $\theta_\triangle$ and may be dependent on the Lipschitz condition on the boundary of Ω. Here $\|f\|_{C(\Omega)}$ is the maximum norm of f over the closed domain Ω and $|f|_{m+1,\Omega} = \max_{\alpha+\gamma=m+1} \|D_x^\alpha D_y^\gamma f\|_{C(\Omega)}$.

We are now ready to study some approximation properties of the spline minimizer in (5). Let us begin with an easy case when f is strictly positive.

Theorem 2.3. *Suppose $z_i = f(x_i, y_i)$, $i = 1, \dots, n$ for a smooth positive function $f \in W_\infty^2(\Omega)$. Let $d \ge 3r+2$ and $\triangle$ be a triangulation of the data sites $\{(x_i; y_i); i = 1; \dots; N\}$. Suppose that $|\triangle|$ is sufficiently small. Then*

$$\|S_z - f\|_{L^2(\Omega)} \le C|\triangle|^2 |f|_{2,\infty,\Omega}, \tag{8}$$

where $C > 0$ is a constant dependent on d and the smallest angle $\rho_\triangle$ of $\triangle$ as well as the Lipschitz constant associated with the boundary $\partial\Omega$ if Ω is not convex.

Proof. A proof follows from the ideas in Lai (2007, 2000). For convenience, we include the detail. Recall Lemma 6.1 from Von Golitschek et al. (2002). That is, suppose g defined on a triangle $T = \langle \mathbf{v}_1; \mathbf{v}_2; \mathbf{v}_3 \rangle$ satisfying $g(\mathbf{v}_i) = 0$ for $i = 1; 2; 3$. Then

$$\|g\|_{\infty,T} \le C|T|^2 |f|_{2,\infty,\Omega} \tag{9}$$

for a constant $C > 0$ dependent on the smallest angle of T. Fix each triangle $T \in \triangle$. Since $g = S_z - f$ is zero at the vertices of T, we have

$$\|S_z - f\|_{\infty,T} \le C|T|^2 |S_z - f|_{2,\infty,\Omega} \le C|T|^2 (|S_z|_{2,\infty,\Omega} + |f|_{2,\infty,\Omega}). \tag{10}$$

Using the stability property of Bernstein–Bézier polynomial S_z over T (see Theorem 1.1 in Lai and Schumaker, 2007) we have

$$|S_z|_{2,\infty,\Omega} \le \frac{K}{A_T^{1/2}} (E(S_z|_T))^{1/2}, \tag{11}$$

where A_T is the area of triangle T and K is a positive constant dependent only on d. It follows that

$$\begin{aligned}
\int_\Omega |S_z - f|^2 dxdy &= \sum_{T\in\triangle} \int_T |S_z - f|^2 dxdy \le \sum_{T\in\triangle} 2C^2|T|^4 A_T (|f|_{2,\infty,T}^2 + \frac{K^2}{A_T} E(S_z|_T)) \\
&\le 2C^2|\triangle|^4 |f|_{2,\infty,\Omega}^2 \sum_{T\in\triangle} A_T + 2C^2|\triangle|^4 K^2 \sum_{T\in\triangle} E(S_z|_T) \\
&= 2C^2|\triangle|^4 |f|_{2,\infty,\Omega}^2 A_\Omega + 2C^2|\triangle|^4 K^2 E(S_z),
\end{aligned}$$

where A_Ω stands for the area of domain Ω.

Note that when $f \ge \epsilon > 0$ over Ω, we use $Q(f)$ from the above theorem to have

$$\min_{(x,y)\in\Omega} Q(f)(x,y) \ge \min_{(x,y)\in\Omega} f(x,y) - \|f - Q(f)\|_{C(\Omega)} \ge \epsilon - K|\triangle|^{m+1} |f|_{m+1,\Omega}.$$

When $|\triangle|$ is small enough, we can have $\min_{(x,y)\in\Omega} Q(f)(x,y) \ge 0$. Note that the construction of $Q(f)$ shows that $Q(f)$ interpolates f at all the vertices of f. Thus, $Q(f) \in U$ and hence, $E(S_z) \le E(Q(f))$.

Furthermore, for $\alpha+\gamma = 2$ in (7) above, we have

$$E(Q(f)) \le 2E(Q(f) - f) + 2E(f) \le 2A_\Omega |Q(f) - f|_{2,\Omega}^2 + 2A_\Omega |f|_{2,\Omega}^2 \le K_1 A_\Omega |f|_{2,\Omega}^2$$

for a positive constant K_1. That is, $E(S_z) \le K_2 |f|_{2,\Omega}^2$ for another positive constant K_2. We now summarize the discussion to conclude the desired approximation property (8) with another positive constant K for $d \ge 3r+2$. □

We continue to discuss the approximation property of S_z. Mainly, we study the approximation of S_z without assuming that f is strictly positive and $|\triangle|$ is sufficiently small. Let us consider the case for $d = 2, 3, 4$ first. As discussed before, we use a Powell–Sabin refinement of a triangulation associated with the data locations. Let $\mathcal{I}_{PS}^+(f)$ be the positive interpolatory spline function from Schumaker and Speleers (2010). The following approximation property was established in Schumaker and Speleers (2010):

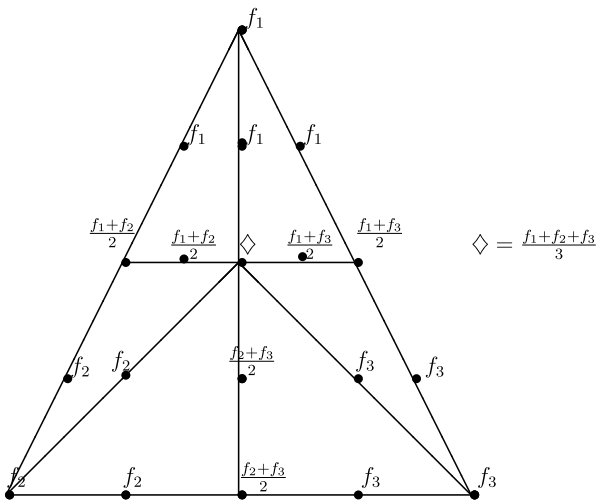

Fig. 4. An example of spline representation over a triangle.

Theorem 2.4. *(See Schumaker and Speleers, 2010.) Suppose f is a nonnegative function in $C^{k+1}(\Omega)$ with $0 \le k \le 2$. For any triangulation $\triangle$ of (x_i, y_i), $i = 1, \cdots, n$, let $PS_\triangle$ be an associated Powell–Sabin refinement of $\triangle$. Then the nonnegative fit $\mathcal{I}_{PS}^+(f)$ of f constructed in Schumaker and Speleers (2010) satisfies*

$$\|f - \mathcal{I}_{PS}^+(f)\|_{\infty,\Omega} \le CL_1(f)|\triangle| + C_2|\triangle|^{k+1}|f|_{k+1,\infty,\Omega}, \tag{12}$$

with $L_1(f)$ being a constant dependent on $|f|_{1,\infty,\Omega}$.

For our application, we need to have an estimate for $\mathcal{I}_{PS}^+(f)$. The inequality in (12) is not very helpful as we have to compute all the second order derivatives of $\mathcal{I}_{PS}^+(f)$ for the evaluation of $E(\mathcal{I}_{PS}^+(f))$ in (5). To do so, let us consider a special nonnegative interpolant $S_{f,0} := \mathcal{I}_{PS}^+(f)$ using $D_x f(\mathbf{v}) = 0 = D_y f(\mathbf{v})$ for all vertices v of $\triangle$. Let us present the Bernstein–Bézier representation of $S_{f,0}$ as in Fig. 4, where the point with barycentric coordinate $(1/2, 1/4, 1/4)$ of a triangle is chosen as the split point P and the line connected to P and the split point of a neighboring triangle intersects the common edge at the middle point of the edge. When the point P is not in such a special location, there will be more ratios of areas of subtriangles shown in the figure. We are now able to calculate $D_{xx}S_{f,0}$ using the B-coefficients shown in Fig. 4.

A straight-forward calculation of $D_{xx}S_{f,0}(x, y)$ at any one subtriangle t of T shows that

$$\begin{aligned}\|D_{xx}S_{f,0}(x,y)\|_{\infty,t} &\le \frac{C}{|t|^2}\max\{|f_1 - f_2|, |f_2 - f_3|, |f_1 - f_3|\}\\ &\le \frac{C_1}{|t|}|f|_{1,\infty,t} \le \frac{C_2}{|T|}|f|_{1,\infty,T}\end{aligned} \tag{13}$$

for a positive constant C_2 dependent on the ratios of subtriangles t and T. Similar for $D_xD_yS_{f,0}(x, y)$ and $D_{yy}S_{f,0}(x, y)$. It follows

$$E(S_{f,0}) = \sum_{T\in\triangle} E(S_{f,0}|_T) \le \sum_{T\in\triangle} \frac{C_2^2 A_T}{|T|^2}|f|_{2,\infty,T}^2 \le \frac{C_2^2 A_\Omega}{|\triangle|^2}|f|_{2,\infty,\Omega}^2$$

for a positive constant $C_3 > 0$ dependent on the β quasi-uniformality of $\triangle$ only. As discussed above, we have

$$\begin{aligned}\int_\Omega |S_z - f|^2 dxdy &\le 2C^2|\triangle|^4|f|_{2,\infty,\Omega}^2 A_\Omega + 2C^2|\triangle|^4K^2E(S_{f,0})\\ &\le 2C^2|\triangle|^4|f|_{2,\infty,\Omega}^2 A_\Omega + 2C^2|\triangle|^2K^2C_3^2A_\Omega|f|_{1,\infty,\Omega}^2.\end{aligned}$$

Hence, we have $\|S_z - f\|_{L^2(\Omega)} \le C|\triangle|^2|f|_{2,\infty,\Omega} + C|\triangle||f|_{1,\infty,\Omega}$. This motivates the following

Theorem 2.5. *Suppose $z_i = f(x_i, y_i)$, $i = 1, \cdots, N$ for a smooth nonnegative function $f \in W_\infty^2(\Omega)$. Let $\triangle_{PS}$ be a Powell–Sabin refinement of a triangulation of the data sites (x_i, y_i), $i = 1, \cdots, N$. The minimizer S_z of (5) in $S_d^1(\triangle_{PS})$ for $d \ge 2$ satisfies*

$$\|S_z - f\|_{L^2(\Omega)} \le K_1|\triangle|^2|f|_{2,\infty,\Omega} + K_2|\triangle||f|_{1,\infty,\Omega}, \tag{14}$$

where K_1, K_2 are positive constants dependent on d, the area A_Ω, and the smallest angle $\rho_\triangle$ of $\triangle$ as well as the Lipschitz constant associated with the boundary $\partial\Omega$ if Ω is not convex.

Similarly, for $d \geq 5$ we use the Bernstein–Bézier representation of $S_{f,0}$ in Fig. 3 to compute $D_{xx}S_{f,0}$ over T. A similar inequality as in (13) can be established based on a straightforward calculation of $D^2_{\mathbf{v}_i-\mathbf{v}_j}S_{f,0}$, $D_{\mathbf{v}_i-\mathbf{v}_j}D_{\mathbf{v}_i-\mathbf{v}_k}S_{f,0}$ and $D^2_{\mathbf{v}_i-\mathbf{v}_k}S_{f,0}$ which can be bounded by $\max\{|f_i - f_j|, |f_i - f_k|, |f_j - f_k|\}$. The rest is done as the same as the proof of Theorem 2.5. Therefore, we have the following

Theorem 2.6. *Suppose $z_i = f(x_i, y_i), i = 1, \cdots, N$ for a smooth nonnegative function $f \in W^2_\infty(\Omega)$. Let $\triangle_{PS}$ be a Powell–Sabin refinement of a triangulation of the data sites $(x_i, y_i), i = 1, \cdots, N$. Suppose that all the edges of $\triangle$ are active. Then the minimizer S_z of (5) in $S^1_d(\triangle)$ for $d \geq 5$ satisfies the approximation property in (14).*

3. The projected gradient method for nonnegative preserving interpolation

We finally discuss how to numerically solve the minimization in (5). Let us first recall a classic method for solution of a general convex constrained minimization: find $\mathbf{c}^* \in U \subset \mathbb{R}^n$, where U is a convex set such that

$$J(\mathbf{c}^*) = \min_{\mathbf{c}\in U} J(\mathbf{c}), \tag{15}$$

where $J(\mathbf{c})$ is a convex functional. Let us motivate this method as follows: suppose we have the kth iterative solution $\mathbf{c}^{(k)} \in U$ for $k \geq 0$. We compute the next iterative solution by solving

$$\mathbf{c}^{k+1} = \arg\min_{\mathbf{c}\in U} \langle \nabla J(\mathbf{c}^{(k)}), \mathbf{c} - \mathbf{c}^{(k)}\rangle + \frac{L}{2}\|\mathbf{c} - \mathbf{c}^{(k)}\|^2. \tag{16}$$

Let P_U be the projection of U, i.e., $P_U(\mathbf{c}) \in U$ for any $\mathbf{c} \in \mathbb{R}^n$. When J is convex and U is a closed convex set, $\mathbf{c}^{k+1}$ can be computed using the projection P_U. This leads to a projected gradient algorithm as follows:

Algorithm 3.1 *(The classic projected gradient algorithm).* For a given initial guess $\mathbf{c}^{(0)}$, find $\mathbf{c}^{k+1} \in \mathbb{R}^n$ such that

$$\mathbf{c}^{(k+1)} := P_U(\mathbf{c} - \mathbf{c}^{(k)} + \frac{1}{L}\nabla J(\mathbf{c}^{(k)})) \tag{17}$$

for $k \geq 0$ until the maximal number of iterations is achieved, where $L > 0$ is a number dependent on the Lipschitz condition of ∇J.

In terms of our spline notation, we let $J(\mathbf{c}) = \mathbf{c}^\top E\mathbf{c}$ be the thin-plate energy functional and $U = \{\mathbf{c} \in \mathbb{R}^n, H\mathbf{c} = 0, I\mathbf{c} = \mathbf{z}, \mathbf{c} \geq 0\}$ be the convex set, where $H\mathbf{c} = 0$ stands for all smoothness conditions, $I\mathbf{c} = \mathbf{z}$ are a collection of all interpolatory conditions, i.e., $S(x_i, y_i) = z_i$ with $\mathbf{c}$ being the spline coefficients of S. In terms of the projected gradient method, we have

Algorithm 3.2 *(Nonnegative spline fitting algorithm).* Start with an initial guess solution, say $\mathbf{c}^{(0)}$ associated with the minimal energy interpolatory spline satisfying (3). For $k \geq 1$, we compute

$$\min\{\langle \nabla J(\mathbf{c}^{(k)}), \mathbf{c} - \mathbf{c}^{(k)}\rangle + \frac{L}{2}\|\mathbf{c} - \mathbf{c}^{(k)}\|^2, \text{ subject to } H\mathbf{c} = 0, I\mathbf{c} = \mathbf{z}, \mathbf{c} \geq 0\} \tag{18}$$

to find $\mathbf{c}^{(k+1)}$. That is, we find $\mathbf{c}^{k+1}$ by the projection

$$\mathbf{c}^{(k+1)} = \arg\min\{\|\mathbf{c}^k - \frac{1}{L}\nabla J(\mathbf{c}^k) - \mathbf{c}\|, \ H\mathbf{c} = 0, I\mathbf{c} = \mathbf{z}, \mathbf{c} \geq 0\} \tag{19}$$

for $k = 0, 1, 2, \cdots$ until the maximal number of iterations is achieved.

It is known that when J is strongly convex, i.e., elliptic (cf. Ciarlet, 1989), the projected gradient method is convergent linearly. See Theorem 8.6-2 in Ciarlet (1989). That is, we say that a minimizing functional J is elliptic if J is differentiable and there exists a positive constant μ such that

$$\langle \nabla J(\mathbf{a}) - \nabla J(\mathbf{b}), \mathbf{a} - \mathbf{b}\rangle \geq \mu\|\mathbf{a} - \mathbf{b}\|^2, \quad \forall \mathbf{a}, \mathbf{b} \in \mathbb{R}^n. \tag{20}$$

One can easily see that the energy functional $J(\mathbf{c}) = E(s)$ is not strongly convex. Indeed, the strong convexity for twice differentiable functional such as J is equivalent to the fact that Hessian of J is positive definite. However, for the data values which are from any linear polynomial, we know that the Hessian of J is singular. Thus, we have to use a more refined convergence result for the projected gradient method.

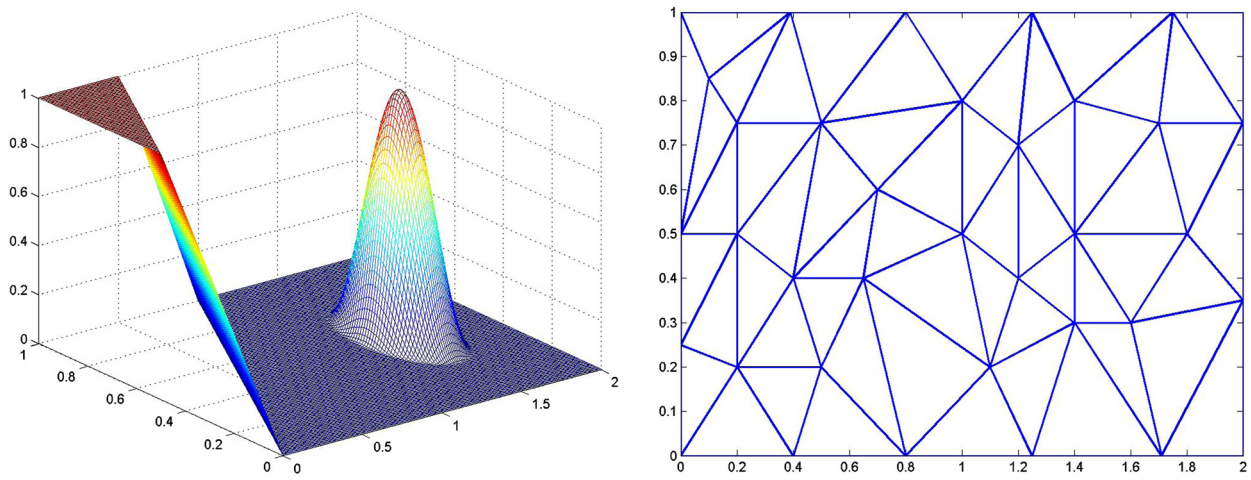

Fig. 5. A nonnegative surface and a triangulation.

Theorem 3.1. *Suppose that the minimization problem (5) has a unique minimizer* $\mathbf{c}^*$. *Suppose that* J *is Lipschitz differentiable. Then the sequence* $\{\mathbf{c}^k, k \geq 1\}$ *from Algorithm 3.1 converges and satisfies*

$$J(\mathbf{c}^k) - J(\mathbf{c}^*) = O(\frac{1}{k}), \quad \forall k \to \infty.$$

We refer to Theorem 4 in Nesterov (2013) for a proof. This explains that our Algorithm 3.2 will converge as it is clear that our J is Lipschitz differentiable. Our Algorithm 3.2 can also be extended to compute the range restricted interpolatory splines. We shall use the projected gradient method to compute the following

$$\min_{s\in S_d^r(\triangle)} \{E(s): \quad s(x_i, y_i) = z_i, i = 1, \cdots, N; A \leq s(x, y) \leq B, \forall (x, y) \in \Omega\}, \tag{21}$$

for any two numbers A, B with $A < B$. See, e.g. Chan and Ong (2001) for study of range-restricted interpolations.

4. Numerical results

4.1. Simulation results

We implemented our Algorithm 3.2 using bivariate spline functions based on MATLAB programs discussed in Awanou et al. (2006) and applied them to several example problems to assess their performance. The major computational step of Algorithm 3.2 is the minimization of the quadratic functional (19), for which we use the Lagrange multiplier method. $\mathbf{c}^{k+1}$ can be solved by using least squares method as the following system of linear equations is not of full rank or by using the iterative method discussed in Awanou et al. (2006):

$$\begin{pmatrix} I & B^\top & H^\top \\ B & 0 & 0 \\ H & 0 & 0 \end{pmatrix} \begin{bmatrix} \mathbf{c}^{k+1} \\ \alpha \\ \gamma \end{bmatrix} = \begin{bmatrix} \mathbf{c}^k - hE\mathbf{c}^{(k)} \\ \mathbf{z} \\ 0 \end{bmatrix}$$

for Lagrange multipliers α and γ, where I is the matrix associated with interpolatory conditions, i.e. $B\mathbf{c} = \mathbf{z}$ with $\mathbf{z}$ being the vector of given function values, and H is the matrix associated with smoothness conditions.

Example 4.1. We begin with an academic example: a given set of data is from the following function:

$$f(x, y) = \begin{cases} 1 & y - x \geq 1/2 \\ 2(y - x) & 0 \leq y - x \leq 1/2 \\ \frac{1}{2}\cos(4\pi\sqrt{(x - 3/2)^2 + (y - 1/2)^2}) + 1/2 & (x - 3/2)^2 + (y - 1/2)^2 \leq 1/16 \\ 0 & \text{otherwise} \end{cases}$$

on the domain $[0, 2] \times [0, 1]$ (cf. Kong et al., 2004; Saaban et al., 2011; Schumaker and Speleers, 2010). A data set and an associated triangulation is shown in Fig. 5. We use bivariate spline space $S_5^1(\triangle)$ to find the standard minimal energy interpolation spline by the algorithm in Awanou et al. (2006) and nonnegative preserving interpolatory spline by our Algorithm 3.2. These two interpolatory surfaces are shown in Fig. 6.

One can see that the minimal energy interpolatory spline method is not able to preserve the nonnegativity. It has negative value as low as -0.13667 while our nonnegative preserving interpolatory spline is nonnegative.

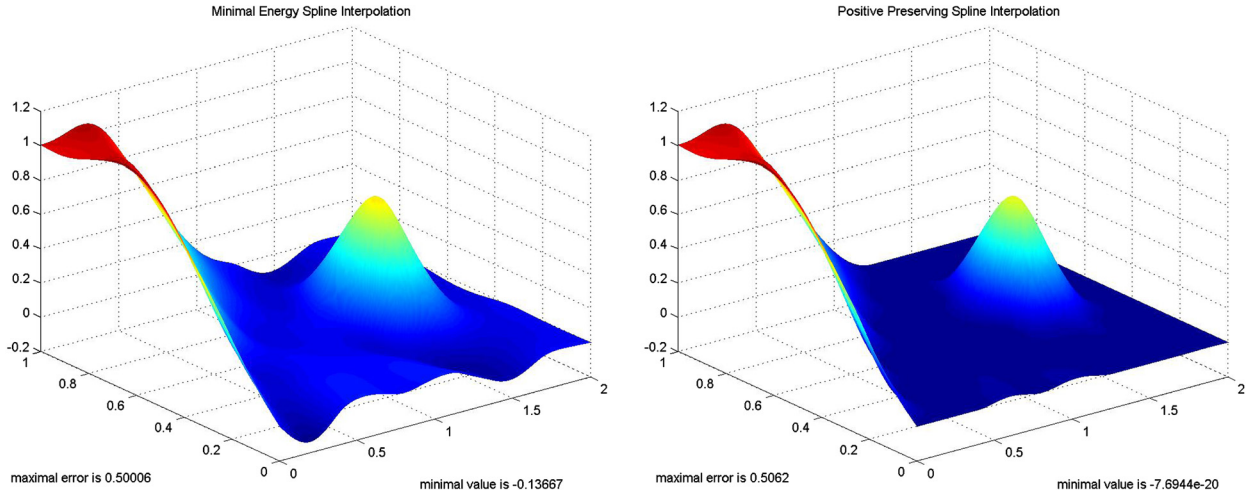

Fig. 6. Minimal energy interpolation and positive preserving interpolation based on triangulation in Fig. 5.

Table 1
Numerical results of range restricted interpolatory splines.

Level of refinement	Min	Max	Accuracy of interpolation	Accuracy of smoothness	Maximum error
0	0	1	1.124e−16	8.710e−5	0.9986
1	0	1	4.422e−16	1.370e−4	0.50843
2	0	1	5.551e−16	2.277e−4	0.13119
3	0	1	1.332e−15	3.621e−4	0.04679
4	0	1	1.221e−15	5.603e−4	0.01126

Table 2
Numerical results of minimal energy interpolatory splines.

Level of refinement	Min	Max	Accuracy of interpolation	Accuracy of smoothness	Maximum error
0	−0.1002	1.0779	9.771e−15	2.564e−14	1.076
1	−0.1242	1.0857	4.851e−14	1.483e−12	0.5118
2	−0.1032	1.046	2.216e−13	1.270e−12	0.1393
3	−0.0327	1.0216	2.658e−12	6.369e−12	0.0496
4	−0.0102	1.0106	1.416e−10	3.260e−10	0.02383

Example 4.2. This is a continuation of Example 4.1. We mainly show how well our nonnegative preserving interpolatory splines can approximate the given nonnegative surface. Similar to an example in Schumaker and Speleers (2010), we first divide the domain $[0,2]\times[0,1]$ into a triangulation $\triangle_0$ of 8 triangles. Then we refine $\triangle_0$ uniformly and repeatedly to have refined triangulations $\triangle_n$, $n=1,2,\cdots,6$. We use C^1 quintic splines in $S_5^1(\triangle_n)$ to approximate the same function f given in Example 4.1 by using both the minimal energy interpolatory spline method and range restricted interpolatory spline method (see the minimization problem in (21)) using the vertices as the data locations and the values of the given function f at these locations. Our numerical results are shown in Tables 1 and 2. We use the accuracy of interpolation, i.e. $\max\{|f(x_i,y_i)-S_f(x_i,y_i)|, i=1,\cdots,N\}$ and the accuracy of smoothness, i.e. the maximum norm of the vector $H\mathbf{c}$ as well as the maximum norm of $f-S_f$ over 201×101 equally-spaced locations to measure how well both spline methods can approximate f.

From the numerical values from Tables 1 and 2 we can see that the range restricted interpolatory splines are able to satisfy the given range restriction and interpolate the given data values with a slight loss of the accuracy of smoothness condition. We looked into detail of the smoothness conditions and saw that all the smoothness conditions are satisfied very well except for those around the bottom of the peak of the surface f, where f is only continuous anyway. This reflects an advantage of our method as the interpolatory spline surface from our approach follows the smoothness pattern of the given data function. Also, our numerical results show that the maximum errors at various levels are consistent with the maximum errors in Schumaker and Speleers (2010). Our method does not need Hermite derivatives at any vertices of underlying triangulation while the methods in Schumaker and Speleers (2010) do. This is another advantage of our method. However, the methods in Schumaker and Speleers (2010) do not require solving a minimization problem which can be expensive for problems of large size.

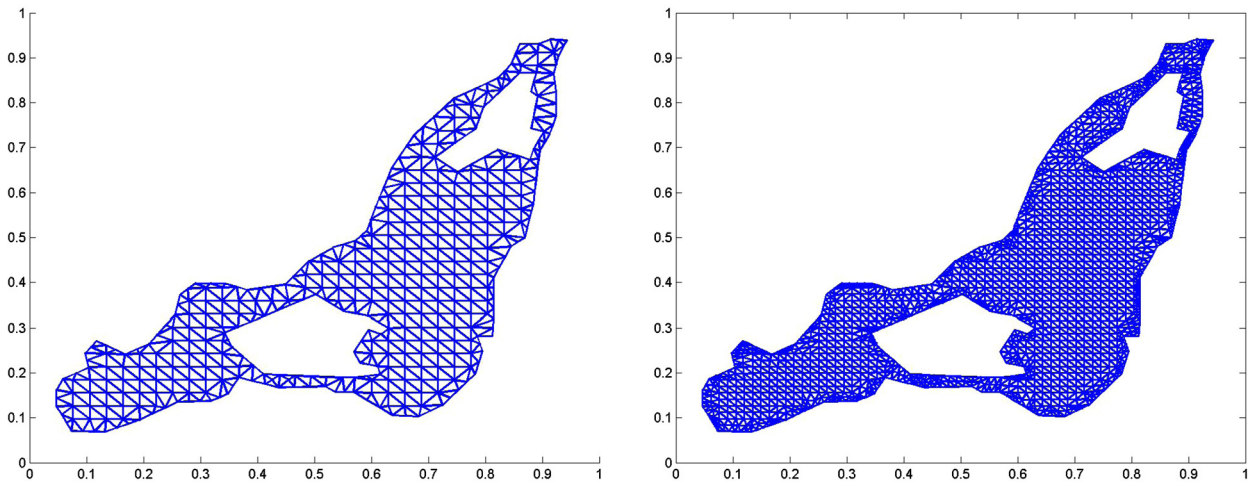

Fig. 7. A triangulation and its uniform refinement of a city.

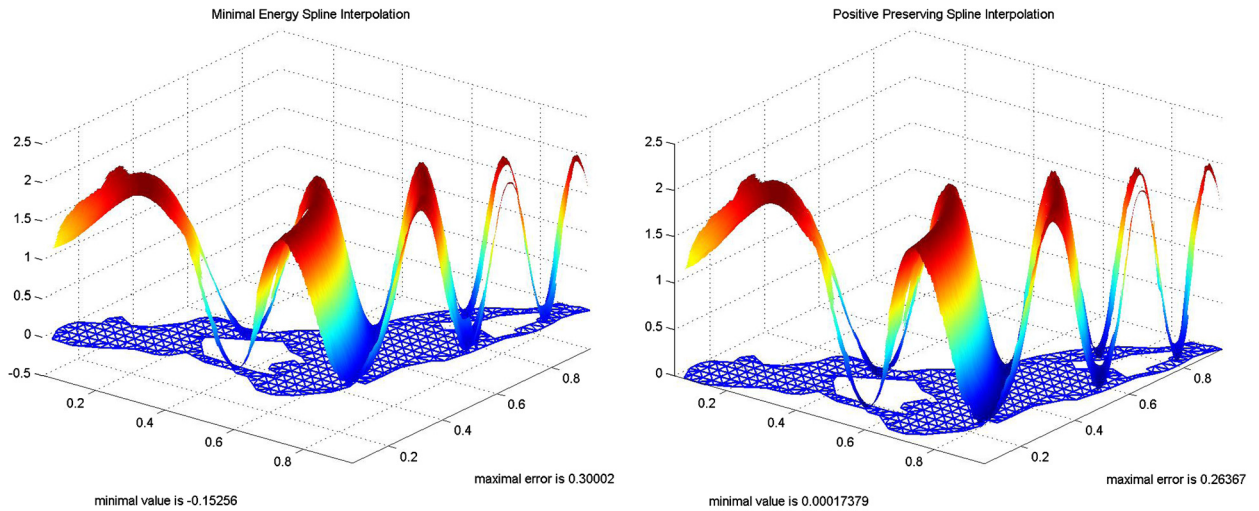

Fig. 8. Minimal energy interpolation and positive preserving interpolation based on triangulation (the left one in Fig. 7).

Example 4.3. In this example, we explain an application of the nonnegative preserving interpolation. Suppose that we are given a set of data values on population density. As the density is a nonnegative function, we can use the method discussed in this paper to generate density distribution from point observations on a complex domain (Fig. 7). We again use the minimal energy interpolatory spline method and nonnegative preserving interpolatory spline method to find interpolatory surfaces of an artificial population density function $f(x, y) = \sin(5\pi(x^2 + y^2)) + 1$. We first use all the vertices of triangulation as data locations. One can see that the minimal energy interpolatory surface has a negative value -0.15256 as in Fig. 8 and -0.005656 as in Fig. 9 over two different triangulations as in Fig. 7 while the nonnegative preserving interpolatory surfaces are indeed nonnegative for both triangulation. Also, the nonnegative preserving interpolatory surface approximates the exact function $f(x, y)$ slightly better in the sense that the maximum error is smaller (0.26367 vs. 0.3000) as shown in Fig. 8 and (0.0001486 vs. 0.01909) as shown in Fig. 9.

In general, we may not be given so many data values at all data locations. The number of vertices in the triangulation (on the left of Fig. 7) is 440. We randomly choose 200 and 300 vertices from the triangulation and find the nonnegative preserving interpolatory surfaces. They are shown in Fig. 10. These surfaces show that the nonnegative preserving interpolatory splines can approximate the exact function well as the number of points increases and the points are distributed over the domain evenly.

4.2. An application to oxygen anomalies in the aftermath of the Deepwater Horizon oil spill

We are now ready to apply our nonnegative preserving interpolatory spline method to deal with real life problems. The Deepwater Horizon oil spill in 2010 injected approximately 4.9 billion barrels of oil (cf. McNutt et al., 2011) and large

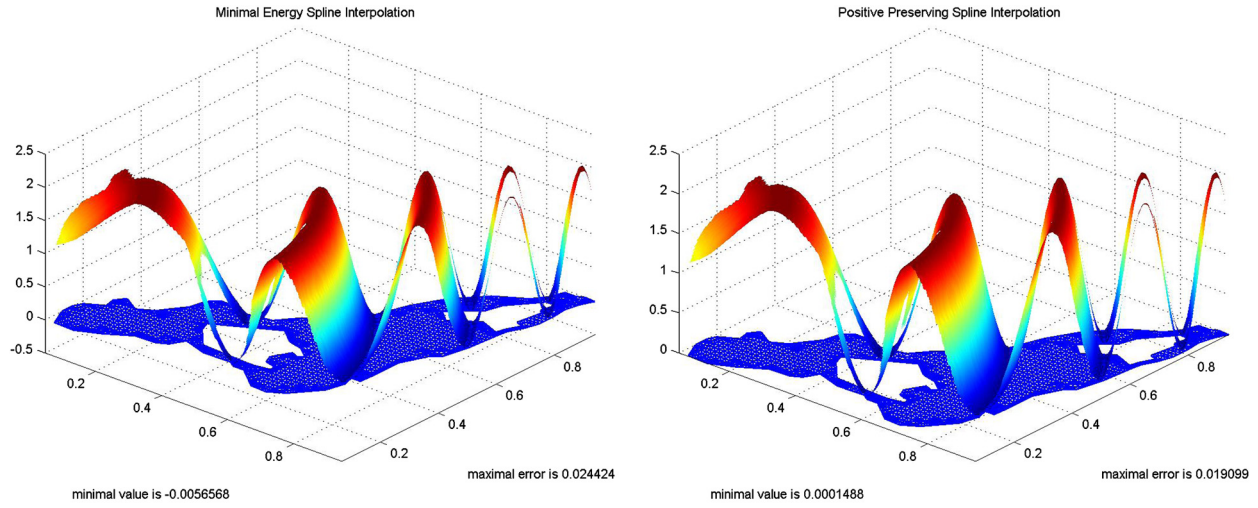

Fig. 9. Minimal energy interpolation and positive preserving interpolation based on triangulation (the right one in Fig. 7).

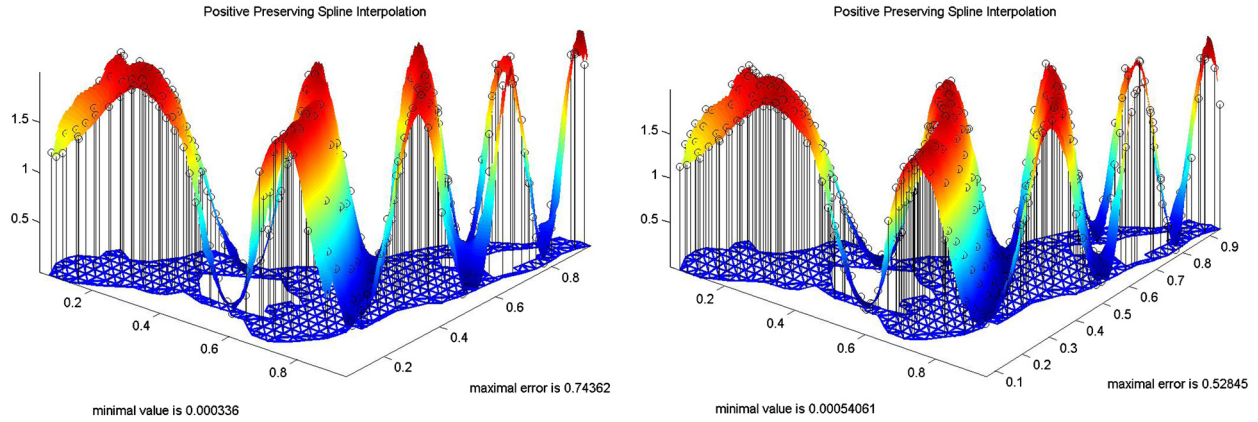

Fig. 10. Positive preserving interpolatory surfaces interpolating at 200 and 300 randomly chosen vertices from the triangulation (the left one in Fig. 7).

quantities of methane (cf. Joye et al., 2011) into Gulf of Mexico deep waters. A fraction of the hydrocarbons injected at a water depth of 1500 m partitioned into the water column (Diercks et al., 2010), with poorly constrained impacts on the deep water ecosystems. The breakdown of hydrocarbons leads to a consumption of molecular oxygen. Analysis of O_2 concentration profiles in the Gulf of Mexico measured in the aftermath of the oil spill allows one to quantify oxygen deficits in the water column, which can be indicative of such decomposition processes. From the measured concentration profiles, O_2 deficits can be determined, resulting in O_2 anomaly profiles that are 0 (no O_2 missing) or positive (indicating O_2 that has been consumed) but – in the absence of O_2 generating processes in the deepwater – never negative. Then, these anomalies were vertically integrated to represent the O_2 deficit in mass per unit surface area. Using standard spatial interpolation techniques, e.g. kriging (cf. Myers, 1994), an estimated 3–3.9 $\times 10^{10}$ moles of O_2 have been consumed in the deep water of the Gulf of Mexico as reported in Kessler et al. (2011). We demonstrate our nonnegative preserving data interpolating scheme by applying it to data collected on the NOAA ship Pisces Cruise IV between August 19 and September 2, 2010, predominantly southwest of the Deepwater Horizon drill site (National Oceanographic Data Center, National Oceanic and Atmospheric Administration).

We first chose a triangulation which fits very tightly the locations where the research vessel collected water column profiles as in Fig. 11. We then manually added additional points to make this triangulation have a better quasi-uniform property (see (4) in order to have a better approximation constant (see Theorem 2.3)).

We constructed a fitting spline with as small variation of the fitting surface as possible and preserving the non-negativity of the interpolatory spline as negative anomalies would indicate a source of O_2, which does not make physical sense. We thus used our Algorithm 3.2 to find such a nonnegative preserving interpolatory spline function of the given oxygen anomaly values.

Example 4.4. We first use a standard minimal energy spline interpolatory method to find the total O_2 anomaly in a layer at a given water depth. We can see that the most negative value of the interpolatory spline surface is very large as shown

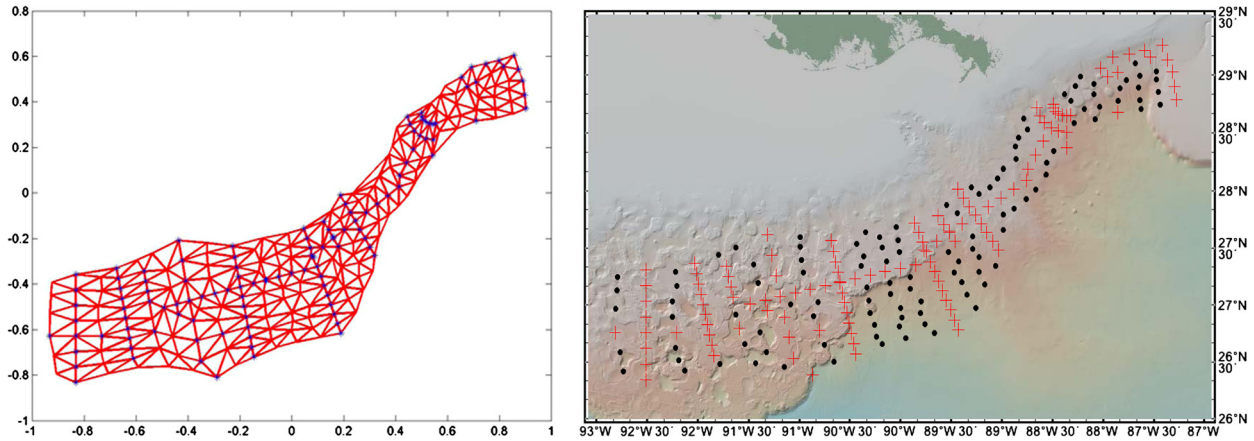

Fig. 11. A triangulation with rescaled measurement locations (in blue dots; left, using scaled coordinates) and an image of the seafloor topography (right, with longitudes and latitudes) with measurement locations (in red crosses) and added vertices (black dots). (For interpretation of the references to color in this figure legend, the reader is referred to the web version of this article.)

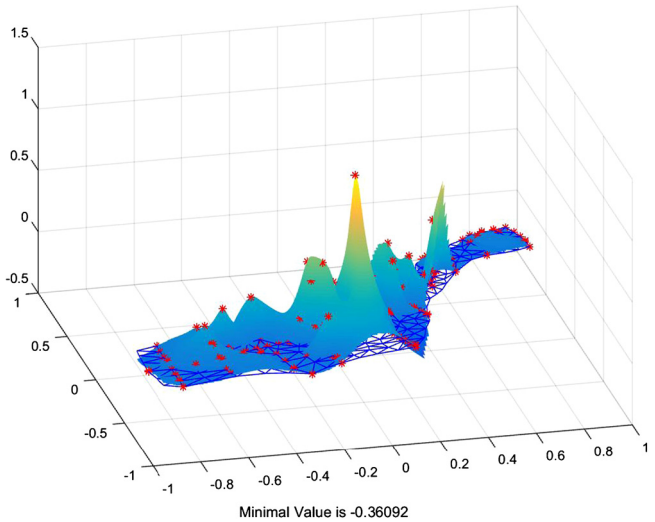

Fig. 12. A minimal energy interpolatory spline surface with negative values as low as -0.36092. The x and y axes denote scaled locations (see Fig. 11, left); The z axis denotes the oxygen anomaly in mg/liter at water depth 1108 meter.

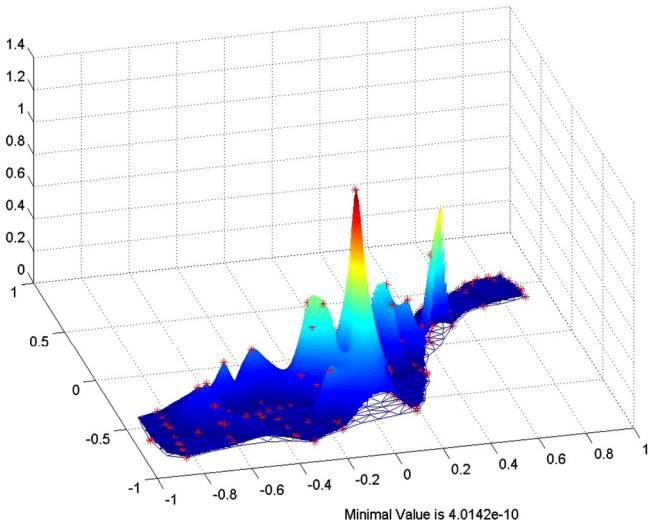

Fig. 13. A nonnegative preserving interpolatory spline surface based on the same scattered data as in Fig. 12.

in Fig. 12. Next let us show the performance of our Algorithm 3.2 in Fig. 13. We can see from that our spline O_2 anomaly surfaces with nonnegative preservation behaves much better than the minimal energy interpolatory method.

In addition, as shown in Fig. 13, we can see that both interpolatory surfaces have no over-shooting and under-shootings in the sense that there are no extreme spline values which are much away from the given data values.

Acknowledgement

CM was supported by the Gulf of Mexico Research Initiative Ecological Impacts of Oil and Gas Inputs to the Gulf. This is ECOGIG contribution #272 and the Pisces data reflect GRIIDC accession number R1.x132.134:0056.

References

Awanou, G., Lai, M.J., Wenston, P., 2006. The multivariate spline method for numerical solution of partial differential equations. In: Chen, G., Lai, M.J. (Eds.), Wavelets and Splines. Nashboro Press, pp. 24–74.

Chan, E.S., Ong, B.H., 2001. Range restricted scattered data interpolation using convex combination of cubic Bézier triangles. J. Comput. Appl. Math. 136, 135–147.

Ciarlet, P., 1989. Introduction to Numerical Linear Algebra and Optimization. Cambridge University Press.

Diercks, A.R., Highsmith, R.C., Asper, V.L., Joung, D., Guo, L., Zhou, Z., Shiller, A.M., Joye, S.B., Teske, A.P., Lohrenz, S.E., 2010. Characterization of subsurface polycyclic aromatic hydrocarbons at the deepwater horizon site. Geophys. Res. Lett. 37, L20602. http://dx.doi.org/10.1029/2010GL045046.

Von Golitschek, M., Lai, M.J., Schumaker, L.L., 2002. Bounds for minimal energy bivariate polynomial splines. Numer. Math. 93, 315–331.

Hussain, M.Z., Hussain, M., 2011. C1 positivity preserving scattered data interpolation using rational Bernstein–Bézier triangular patch. J. Appl. Math. Comput. 35, 281–293.

Joye, S.B., MacDonald, I.R., Leifer, I., Asper, V., 2011. Magnitude and oxidation potential of hydrocarbon gases release from the BO oil well blowout. Nat. Geosci. 4, 160–164.

Kessler, J.D., et al., 2011. A persistent oxygen anomaly reveals the fate of spilled methane in the deep gulf of Mexico. Science 331, 312–315.

Kong, V.P., Ong, B.H., Saw, K.H., 2004. Range restricted interpolation using cubic Bézier triangles. In: Proc. of Computer Graphics, Visualization and Computer Vision. Science Press, Union Agency, Plazen, pp. 125–132.

Lai, M.J., 2000. Convex preserving scattered data interpolation using bivariate C^1 cubic splines. J. Comput. Appl. Math. 119 (1–2), 249–258.

Lai, M.J., 2007. Convergence of three L^1 spline methods for data interpolation and fitting. J. Approx. Theory 145, 196–211.

Lai, M.J., 2008. Multivariate Splines for data fitting and approximation. In: Neamtu, M., Schumaker, L.L. (Eds.), The Conference Proceedings of the 12th Approximation Theory. San Antonio. Nashboro Press, pp. 210–228.

Lai, M.J., Schumaker, L.L., 2007. Spline Functions over Triangulations. Cambridge University Press.

Lai, M.J., Schumaker, L.L., 2009. Domain decomposition method for scattered data fitting. SIAM J. Numer. Anal. 47, 911–928.

McNutt, M., Camilli, R., Guthrie, G., Hsieh, P., Labson, V., Lehr, B., Maclay, D., Ratzel, A., Sogge, M., 2011. Assessment of flow rate estimates for the deepwater horizon/macondowell oil spill. Flow Rate Technical Group report to the National Incident Command. Interagency Solutions Group.

Myers, D., 1994. Spatial interpolation: an overview. Geoderma 62, 17–28.

National Oceanographic Data Center, National Oceanic and Atmospheric Administration. www.nodc.noaa.gov/General/DeepwaterHorizon/ships.html# pisces.

Nesterov, Y., 2004. Introductory Lectures on Convex Optimization. Kluwer Academic Publishers, Boston/Dordrecht/London.

Nesterov, Y., 2013. Gradient methods for minimizing composite functions. Math. Program., Ser. B 140, 125–161.

Saaban, A., Piah, A.R.M., Majid, A.A., 2011. Performance of the triangulation-based methods of positivity-preserving scattered data interpolation. Far East J. Math. Sci. 57 (1), 1–11.

Sarfraz, M., Hussain, M.Z., Ali, M.A., 2012. Positivity-preserving scattered data interpolation scheme using the side-vertex method. Appl. Math. Comput. 218 (15), 7898–7910.

Schumaker, L.L., Speleers, H., 2010. Nonnegativity preserving macro-element interpolation of scattered data. Comput. Aided Geom. Des. 27 (3), 245–261.

Willemans, K., Dierckx, P., 1995. Nonnegative surface fitting with Powell–Sabin splines. Numer. Algorithms 9, 263–276.